

# We are IntechOpen, the world's leading publisher of Open Access books Built by scientists, for scientists

6,900

Open access books available

185,000

International authors and editors

200M

Downloads

Our authors are among the

154

Countries delivered to

TOP 1%

most cited scientists

12.2%

Contributors from top 500 universities



WEB OF SCIENCE™

Selection of our books indexed in the Book Citation Index  
in Web of Science™ Core Collection (BKCI)

Interested in publishing with us?  
Contact [book.department@intechopen.com](mailto:book.department@intechopen.com)

Numbers displayed above are based on latest data collected.  
For more information visit [www.intechopen.com](http://www.intechopen.com)



# Synthesis and Characterization of Amorphous and Hybrid Materials Obtained by Sol-Gel Processing for Biomedical Applications

Catauro Michelina and Bollino Flavia

*Department of Aerospace and Mechanical Engineering,  
Second University of Naples, Aversa,  
Italy*

## 1. Introduction

An interesting research field with medical applications is represented today by ceramics, as they can be used to obtain useful biomaterials for the production of implants (Vallet-Regí, 2001, 2006a, 2006b, 2006c); many parts of the human body, in fact, can be replaced or repaired with biomaterials and more specifically with bioceramics (Black & Hastings, 1998). Regardless of the ceramic type and the application procedure, the introduction of an implant in a living body always causes inflammation phenomena and frequently infection processes as well. Those problems can be overcome by using local drug delivery methods to confine pharmaceuticals such as antibiotics, anti-inflammatory, anti-carcinogens, etc. (Arcos et al., 2001; Ragel & Vallet-Regí, 2000; Vallet-Regí et al., 2000). The possibility of introducing certain drugs into the ceramic matrices employed for bone and teeth repair is undoubtedly an added value to be taken into account.

The traditional use of high temperature procedures to model glasses and ceramics to the desired shape is very well known; on the other hand, the degradation temperature of a pharmaceutical compound is usually around 100°C, which is very low if compared with the high ones needed to compact the components (around 1000°C). Consequently, the main problem is how to include pharmaceuticals in conventional glass and ceramic implants. The scientific community is currently investigating new procedures to incorporate drugs into implantable biomaterials.

The sol-gel process, among others, has proved to be a versatile one and has been widely used in the preparation of amorphous and or hybrid materials (Hench & West, 1990; Judeinstein & Sanchez, 1996; Novak, 1993), with applications, for example, in non-linear optical materials (Hsiue et al., 1994) and mesoporous materials (Wei et al., 1999). The family of organic-inorganic hybrid materials has attracted considerable attention because of its interesting properties such as molecular homogeneity, transparency, flexibility and durability. A key issue that remains unresolved in these organic-modified materials is the degree of mixing of the organic-inorganic components, i.e., phase homogeneity. The high optical transparency to visible light indicates that the organic-inorganic phase separation, if any, is on a scale of  $\leq 400\text{nm}$ . Such hybrids are promising materials for various applications, e.g.: solid state lasers (optical components), replacements for silicon dioxide as insulating materials in the

microelectronic industry, anti-corrosion and scratch resistant coatings, contact lenses or host materials for chemical sensors. In the recent years interest in those materials is connected to their possible applications as biomaterials (Gigant et al., 2002; Joshua et al., 2001; Klukowska et al., 2002; Mackenzie & Bescher, 1998; Matsuura et al., 2001; Spanhel et. al., 1995). One indirect advantage of including polymers is that it is possible to obtain synergistic effects that combine the best properties of polymers with the best properties of inorganic materials. These materials are considered as biphasic materials, where the organic and inorganic phase is mixed at the nm to sub-µm scales. Nevertheless, it is obvious that the properties of these materials are not just the sum of the individual contributions from both phases; the role of the inner interfaces could be predominant. The nature of the interface has recently been used to divide these materials into two distinct classes (Sanchez & Ribot, 1994). In class I, organic and inorganic compounds are embedded and only the weak bonds (hydrogen, van der Waals bonds) give the cohesion to the whole structure. In class II materials, the phases are linked together through strong chemical bonds (covalent or ionic-covalent bonds). Both class I and class II hybrids were prepared by sol-gel technique (Young, 2002).

The aim of the present chapter is to summarize the synthesis via sol-gel and the characterisation methods of amorphous and hybrid materials for biomedical applications. Therefore, the emphasis of our discussion will be focussed on the science, rather than on the technology, of sol-gel processing. The controlled release of pharmaceuticals such as anti-inflammatory agents and antibiotics from strong and biocompatible hosts has relevant applications: they include implantable therapeutic systems, filling materials for bone or teeth repair, which curtail inflammatory or infectious side effects of implant materials when coatings of biocompatible materials containing anti-inflammatory or antibiotic drugs are applied.

2. General processing methods

Different types of colloids can be used to produce polymers or particles from which we can obtain a ceramic material: for example, sols (suspensions of solid particles in a liquid), aerosols (suspensions of particles in a gas) or emulsions (suspensions of liquid droplets in another liquid). The sol-gel chemistry is based on the hydrolysis and polycondensation of molecular precursors such as metal alkoxides  $M(OR)_x$ , where  $M = Si, Sn, Ti, Zr, Al, Mo, V, W, Ce$  and so forth. The following sequence of reactivity is usually found as  $Si(OR)_4 \ll Sn(OR)_4 = Ti(OR)_4 < Zr(OR)_4 = Ce(OR)_4$  (Novak, B.M.,1993 ). Fig. 1 presents a schema of the procedures which one could follow within the scope of sol-gel processing. In the sol-gel process, the precursors for the preparation of a colloid consist of a metal or metalloid element surrounded by various ligands. A list of the most commonly used alkoxy ligands is presented in Tab. 1.

Alkyl		Alkoxy	
methyl	●CH <sub>3</sub>	Methoxy	●OCH <sub>3</sub>
ethyl	●CH <sub>2</sub> CH <sub>3</sub>	Ethoxy	●OCH <sub>2</sub> CH <sub>3</sub>
n-propyl	●CH <sub>2</sub> CH <sub>2</sub> CH <sub>3</sub>	n-propoxy	●OCH <sub>2</sub> CH <sub>2</sub> CH <sub>3</sub>
Iso-propyl	H <sub>3</sub> C(●C)HCH <sub>3</sub>	Iso-propyl	H <sub>3</sub> C(●O)CHCH <sub>3</sub>
n-butyl	●CH <sub>2</sub> (●CH <sub>2</sub> ) <sub>2</sub> CH <sub>3</sub>	n-butoxy	●O(CH <sub>2</sub> ) <sub>3</sub> CH <sub>3</sub>
Sec-butyl	H <sub>3</sub> C(●C)HCH <sub>2</sub> CH <sub>3</sub>	Sec- propoxy	H <sub>3</sub> C(●O)CHCH <sub>2</sub> CH <sub>3</sub>
Iso- butyl	●CH <sub>2</sub> CH(CH <sub>3</sub> ) <sub>2</sub>	Iso- propoxy	●OCH <sub>2</sub> CH(CH <sub>3</sub> ) <sub>2</sub>
Tert-butyl	●C(CH <sub>3</sub> ) <sub>3</sub>	Tert- propoxy	●OC(CH <sub>3</sub> ) <sub>3</sub>

Table 1. Commonly used ligands in sol-gel process.

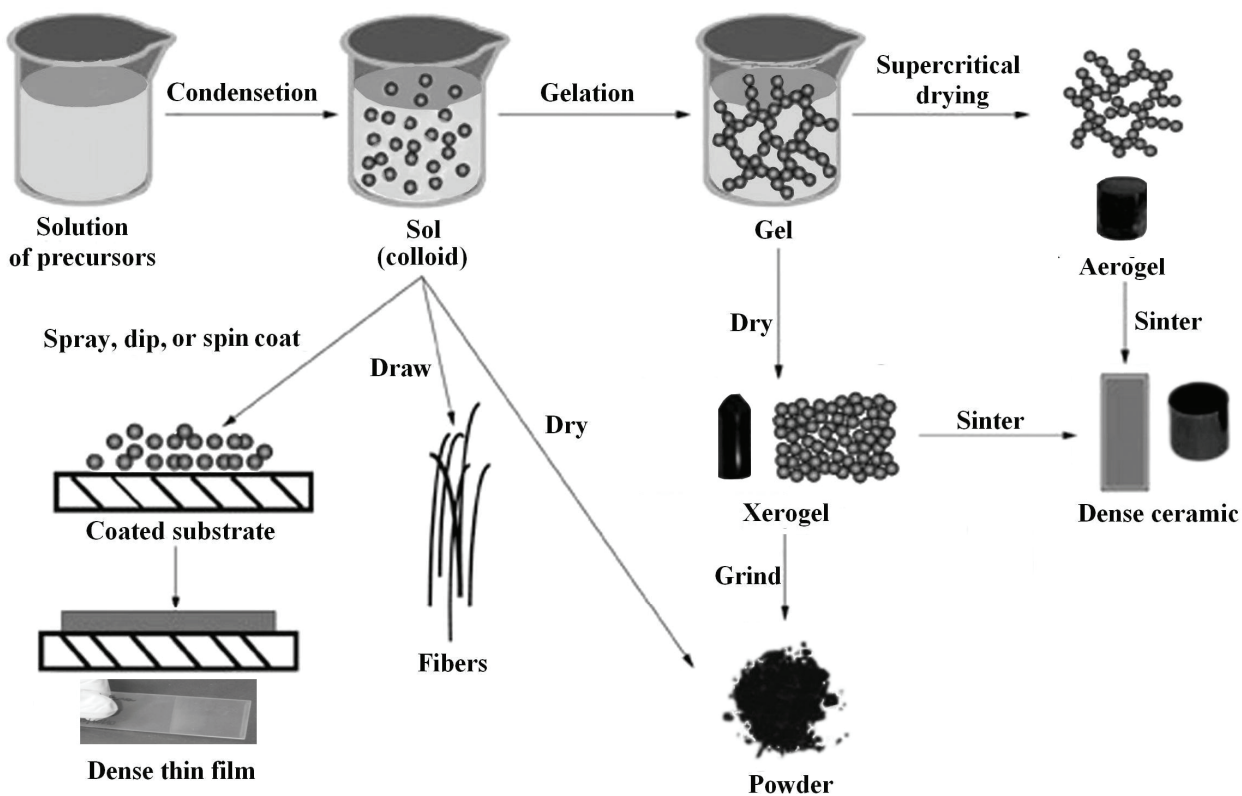
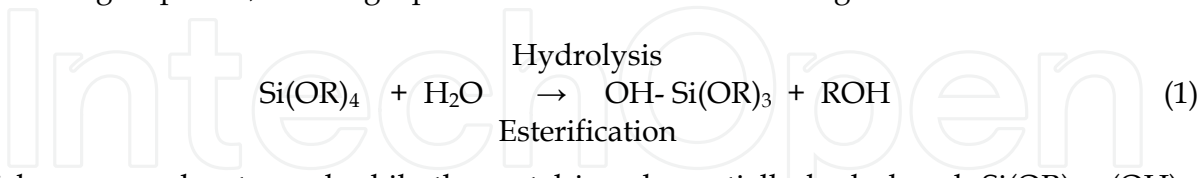


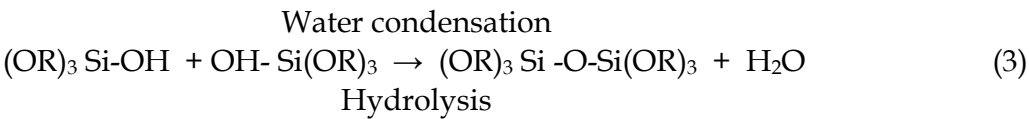
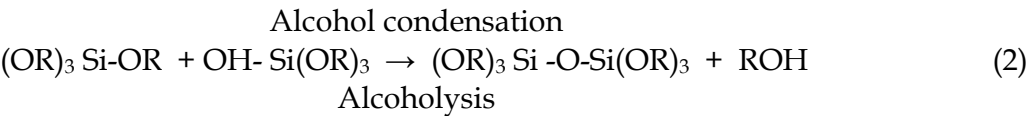
Fig. 1. Schematic of sol-gel processing.

2.1 Hydrolysis and condensation

The alkoxydes used as ligands can be organometallic compounds, where direct metal-carbon bonds are present, or also members of the family or metalloid atoms, the so called metal alkoxydes, among which the most widely known, as it has been extensively studied, is the silicon tetraethoxide (or tetrathoxy-silane, or tetraethyl orthosilicate, TEOS),  $\text{Si}(\text{OC}_2\text{H}_5)_4$ . Silicate gels are most often synthesized by hydrolyzing monomeric, tetrafunctional alkoxyde precursors employing a mineral acid (e.g., HCl) or base (e.g.  $\text{NH}_3$ ) as a catalyst. At the functional group level, the sol-gel process starts with the following reaction:



which can even be stopped while the metal is only partially hydrolyzed,  $\text{Si}(\text{OR})_{4-n}(\text{OH})_n$ . Then, two partially hydrolyzed molecules can link together in a condensation reaction, such as one of the following:



where R is an alkyl group,  $C_xH_{2x+1}$ . The hydrolysis reaction (eq. 1) replaces alkoxide group (OR) with hydroxyl group (OH). Subsequent condensation reactions involving the silanol group produce siloxane bonds (Si-O-Si) and the by-products alcohol (ROH) (eq. 2) or water (eq. 3). Under most conditions, condensation starts (eqs. 2 and 3) before hydrolysis (eq. 1) is complete. A solvent such as an alcohol is normally used as a homogenizing agent, as water and alkoxysilanes are immiscible (Fig. 2). However, a gel can be prepared from silicon alkoxide-water mixtures without adding a solvent (Avnir & Kaufman, 1987), since the alcohol produced as the by-product of the hydrolysis reaction is sufficient to homogenize the initially phase separated system. It should be noted that the alcohol is not simply a solvent. As indicated by the reverse of eqs. 1 and 2, it can participate in esterification or alcoholysis reactions.

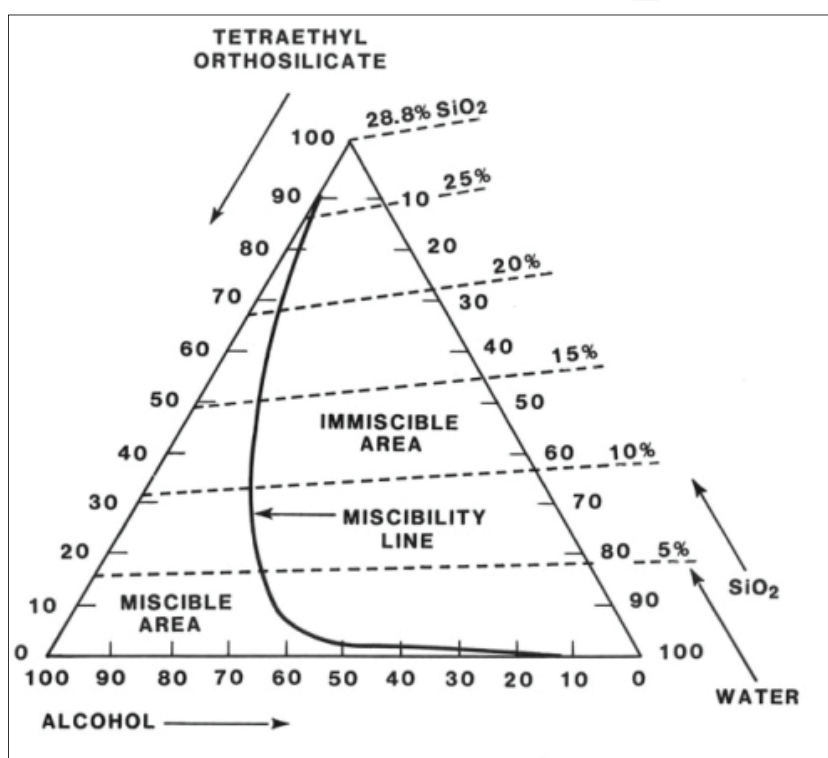


Fig. 2. TEOS,  $H_2O$ , Synasol (95% EtOH, 5% water) ternary-phase diagram at  $25^\circ C$ . For pure ethanol the miscibility line is slightly shifted to the right (Cologan & Setterstrom, 1946).

The  $H_2O:Si$  molar ratio ( $r$ ) in eq. 1 has been made to vary from less than one to over 50, and the concentration of acid or bases from less than 0.01 (Brinker et al., 1982) to 7M (Stober et al., 1968) depending on the desired end product. Typical gel-synthesis procedures used to produce bulk gels, films, fibres, and powders are listed in Tab 2. Hydrolysis occurs by the nucleophilic attack of the oxygen contained in water on the silicon atom as shown by the reaction of isotopically labelled water with TEOS that produces only unlabelled alcohol in both acid-base-catalyzed systems (Voronkov & et al., 1978). Hydrolysis is facilitated in the presence of homogenizing agents (alcohols, dioxane, THF, acetone, etc.) that are especially beneficial in promoting the hydrolysis of silanes containing bulk organic or alkoxy ligands. It should be emphasized, however, that the addition of solvents may promote esterification or depolymerization reactions according to the reverse of eqs. 1 and 2.

SiO <sub>2</sub> Gel Types	% Mole					
	TEOS	EtOH	H <sub>2</sub> O	HCl	NH <sub>3</sub>	H <sub>2</sub> O/Si(r)
Bulk	6.7	25.8	67.3	0.2	-	10
Fibers	11.31	77.26	11.31	0.11	-	1.0
Films	5.32	36.23	58.09	0.35	-	10.9
Monodisperse Spheres	0.83	33.9	44.5	-	20.75	53.61

Table 2. Sol-gel Silicate compositions for bulk gels, fibres, film and powder.

The Hydrolysis is more rapid and complete when catalysts are employed (Voronkov et al., 1978). Although mineral acids or ammonia are most generally used in sol-gel processing, other known catalysts are acetic acid, KOH, amines , KF, HF, titanium alkoxides, and vanadium alkoxides and oxides (Voronkov et al , 1978). In the literature mineral acids are reported to be more effective catalysts than the equivalent base concentrations. However, neither the increasing acid of silanol groups with the extent of hydrolysis and condensation (Keefer, 1984) nor the generation of unhydrolyzed monomers via base-catalyzed alcoholic or hydrolytic depolymerization processes have generally been taken into account. Aelion et al., (1950a, 1950b) investigated the hydrolysis of TEOS under acid and basic conditions using several cosolvents: ethanol, methanol, and dioxane. The extent of hydrolysis (eq. 1) was determined by distillation of the ethanol by-product. Karl Fischer titration was used to follow the consumption of water by hydrolysis (eq.1) and its production by condensation (eq.3). Aelion et al. observed that the rate and extent of the hydrolysis reaction was mostly influenced by the strength and concentration of the acid or base catalyst. As under acid conditions, the hydrolysis of TEOS in base media was a function of the catalyst concentration (Aelion et al., 1950a, 1950b).

Steric (spatial) factors exert the greatest effect on the hydrolytic stability of organoxysilanes (Voronkov et al., 1978). Any complication of the alkoxy group delays the hydrolysis of alkoxy silanes, but the hydrolysis rate is lowered at most by the branched alkoxy group (Voronkov et al., 1978). The effects of alkyl length and the degree of branching observed by (Aelion et al., 1950a, 1950b) are illustrated in Tab. 3 for the hydrolysis of tetralkoxysilanes.

R	k 10 <sup>2</sup> (1 mol <sup>-1</sup> s <sup>-1</sup> [H <sup>+</sup> ] <sup>-1</sup> )
C <sub>2</sub> H <sub>5</sub>	5.1
C <sub>4</sub> H <sub>9</sub>	1.9
C <sub>6</sub> H <sub>13</sub>	0.83
(CH <sub>3</sub> ) <sub>2</sub> CH(CH <sub>2</sub> ) <sub>3</sub> CH(CH <sub>3</sub> )CH <sub>2</sub>	0.30

Table 3. Rate constant k for acid hydrolysis of tetralkoxysilanes (RO)<sub>4</sub>Si at 20°C

Fig. 3 compares the hydrolysis of TEOS and TMOS under acid and basic conditions. The delaying effect of the bulkier ethoxide group is clearly evident. According to (Voronkov et al., 1978) in the case of mixed alkoxides, (RO)<sub>x</sub>(R'O)<sub>4-x</sub>Si where R'O is a higher (larger) alkoxy group than RO, if the R'O has a normal (i.e. linear) structure, its retarding effect on the hydrolysis rate is manifest only when x= 0 or 1. If R'O is branched, its delaying effect is evident even when x= 2. The hydrolysis of the n-propoxide group was observed to be slower than the ethoxide group during the second hydrolysis step under both acid and basic conditions. This result suggests that a delaying effect of a higher, normal alkoxide group is realized regardless of the extent of substitution.

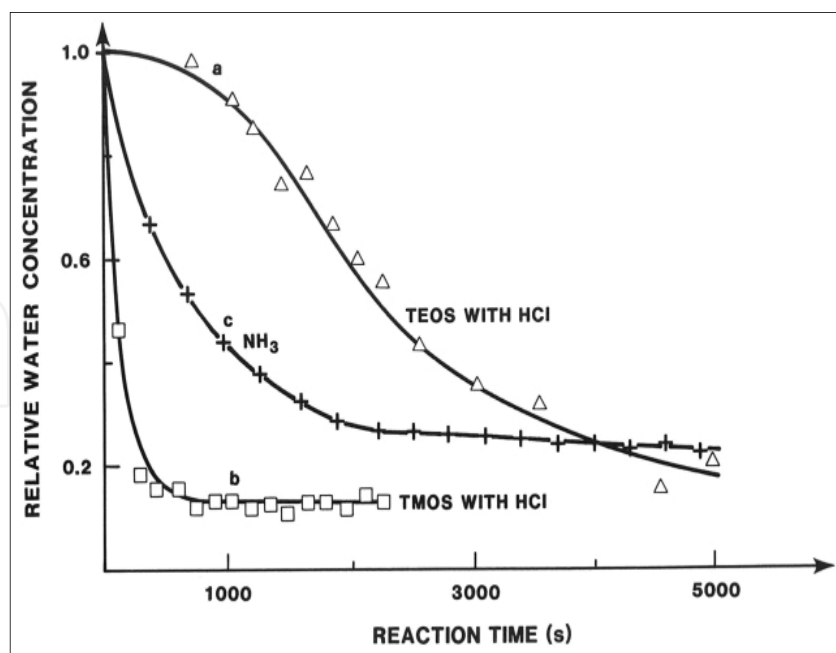


Fig. 3. Relative water concentration versus time during acid- or base-catalyzed hydrolysis of  $\square$ : TMOS with HCl ;  $\times$ : TEOS and TMOS with  $\text{NH}_3$ .  $\Delta$ : TEOS with HCl (Shih et al., 1987)

The substitution of one alkyl group with alkoxy groups increases the electron density on the silicon. Conversely, hydrolysis (substitution of OH for OR) or condensation (substitution of OSi for OR or OH) decreases the electron density on the silicon Fig. 4. Inductive effects are evident from investigations on the hydrolysis of methylethoxysilanes (Schmidt et al., 1984),  $(\text{CH}_3)_x(\text{C}_2\text{H}_5\text{O})_{4-x}\text{Si}$  where  $x$  varies from 0 to 3. Fig. 5 shows that under acidic (HCl) conditions, the hydrolysis rate increases with the degree of substitution  $x$ , of electron-providing alkyl group, whereas under basic ( $\text{NH}_3$ ) conditions the reverse trend is clearly observed.

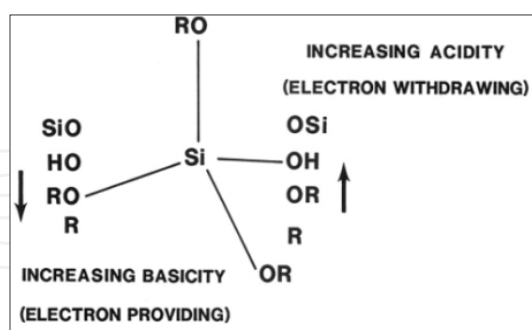


Fig. 4. Inductive effects of substituents attached to silicon, R, OR, OH or OSi (Brinker, 1988)

Fig. 5 also shows the accelerating effect of methoxide substitution on the hydrolysis rate (TMOS versus TEOS). The acceleration and retardation of hydrolysis with increasing  $x$  under acid and basic conditions respectively, suggest that the hydrolysis mechanism is sensitive to inductive effects and is apparently unaffected by the extent of alkyl substitution. Because increased stability of the transition state will increase the reaction rate, the inductive effects are evident for positively and negatively charged transition states or intermediates under acid and basic conditions respectively. This reasoning leads to the hypothesis that

under acid conditions, the hydrolysis rate decreases with each subsequent hydrolysis step (electron withdrawing), whereas under basic conditions the increased electron-withdrawing capabilities of OH (and OSi) compared to OR may establish a condition in which each subsequent hydrolysis step occurs more quickly as hydrolysis and condensation proceed.

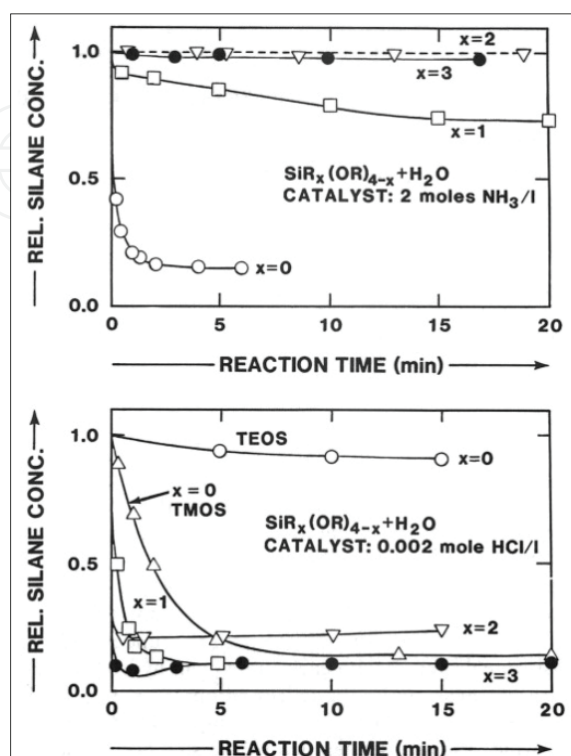


Fig. 5. Relative silane concentration versus time during acid- and base-catalyzed hydrolysis of different silanes in ethanol (volume ratio to EtOH=1:1). ●:  $(\text{CH}_3)_3\text{SiOC}_2\text{H}_5$ .

▽:  $(\text{CH}_3)_2\text{Si}(\text{OC}_2\text{H}_5)_2$ . □:  $(\text{CH}_3)_2\text{Si}(\text{OC}_2\text{H}_5)_3$ . ○:  $\text{Si}(\text{OC}_2\text{H}_5)_4$ . Δ:  $\text{Si}(\text{OCH}_3)_4$ . (Shih et al., 1987)

From the standpoint of organically modified alkoxy silanes,  $\text{R}_x\text{Si}(\text{OR})_{4-x}$ , the inductive effects indicate that acid-catalyzed conditions are preferable (Schmidt et al., 1984), since acids are effective in promoting hydrolysis both when  $x=0$  and  $x>0$ . As indicated in Tab. 2, the hydrolysis reaction has been performed with  $r$  values ranging from  $<1$  to over 25 depending on the desired polysilicate product, for example, fibers, bulk gel or colloidal particles. From eq. 1, an increased value of  $r$  is expected to promote the hydrolysis reaction. (Aelion et al., 1950a, 1950b) found the acid-catalyzed hydrolysis of TEOS to be first-order in  $[\text{H}_2\text{O}]$ ; however, they observed an apparent zero-order dependence of the water concentration under base-catalyzed conditions. As explained, this is probably due to the production of monomers by siloxane bond hydrolysis and redistribution reactions.

Solvents are usually added to prevent liquid-liquid phase separation during the initial stages of the hydrolysis reaction and to control the concentrations of silicate and water that influence the gelation kinetics. More recently, the effects of solvents have been studied primarily in the context of drying control chemical additives (DCCA) used as cosolvents with alcohol in order to facilitate rapid drying of monolithic gels without cracking (Hench et al., 1986). Solvents can be classified as polar or nonpolar and as protic or aprotic. The dipole moment of a solvent determines the length over which the charge of one species can be "felt" by surrounding species. The lower the dipole moment, the larger this length becomes. This



they progressively become connected to the network and the stiffness of the gel will increase. The gel appears when the last link is formed between two large clusters to create the spanning cluster. This bond is no different from innumerable others that form before and after the gel point, except that it is responsible for the onset of elasticity by creating a continuous solid network. The sudden change in rheological behaviour is generally used to identify the gel point in a crude way.

The classic theory explains the theory developed by Flory (1953) and Stockmayer (1945) to account for the gel point and the molecular-weight distribution in the sol. The most important deficiency of this model is that it neglects the formation of closed loops within the growing clusters, and this leads to unrealistic predictions about the geometry of the polymers. The percolation theory offers a description that does not exclude the formation of closed loops and so does not predict a divergent density for large clusters. The disadvantage of the theory is that it generally does not lead to analytical solutions for such properties as the percolation threshold or the size distribution of polymers. However, these features can be determined with great accuracy from computer simulations, and the results are often quite different from the predictions of the classical theory. Excellent reviews of percolation theory and its relation to gelation have been written by Zallen (1983) and Stauffer et al. (1982); and the kinetic models are based on Smoluchowski's analysis of the growth and aggregation of clusters.

The Smoluchowski equation describes the rate at which the number,  $n_s$ , of clusters of size  $s$  changes with time  $t$ , during an aggregation process :

$$\frac{dn_s}{dt} = \frac{1}{2} \sum_{i+j=s} K(i,j)n_i n_j - n_s \sum_{j=1}^{\infty} K(s,j)n_j \quad (5)$$

The coagulation kernel,  $K(i,j)$  is the rate coefficient for aggregation of a cluster of size  $i$  with another and of size  $j$ . The first term in eq. 5 gives the rate of creation of size  $s$  by aggregation of two smaller clusters, and the second term gives the rate at which clusters of size  $s$  are eliminated by further aggregation. For this equation to apply, the sol must be so diluted that collisions between more than two clusters can be neglected, and the clusters must be free to diffuse so that the collisions occur at random. Further, since  $K$  depends only on  $i$  and  $j$ , ignoring the range of structures that could be present in a cluster of a given size, this is a mean-field analysis that replaces structural details with averages.

### 2.3 Drying

The drying of a porous material is a process which can be divided into several stages. At first the body shrinks by an amount equal to that volume of the evaporated liquid and the liquid-vapor interface remains at the exterior surface of the body. The second stage begins when the body becomes too stiff to shrink and the liquid recedes into the interior, leaving air-filled pores near the surface. Even as air invades the pores, a continuous liquid film supports flow to the exterior, so evaporation continues to occur from the surface of the body. Eventually, the liquid becomes isolated into pockets and drying can proceed only by evaporation of the liquid within the body and diffusion of the vapor to the outside. In the specialized literature the factors affecting stress development are discussed and various strategies to avoid warping and cracking are described. The outline is as follows:

- Phenomenology
- Drying stress
- Avoiding fracture

The first stage of drying is called the constant rate period (CRP), because the rate of evaporation per unit area of the drying surface is uniform (Fortes & Okos, 1980; Macey, 1942; Moore, 1961). The evaporation rate is close to that of an open dish of liquid, as indicated by the data for the drying of alumina gel (Dwivedi, 1986), shown in Fig. 6. The rate may differ slightly, depending on the texture of the surface. For example, as sand beds dry, the water conforms to the shapes of the particles, so the wet area is larger than the planar one pertaining to the surface of the body, and the rate of evaporation is correspondingly higher (Ceaglske & Hougen, 1937). The distribution of a spreading liquid is illustrated schematically in Fig.6. The chemical potential,  $\mu$ , of the liquid in the adsorbed film is equal to the one under the concave meniscus, otherwise liquid would flow from one to the other to balance the potential. The chemical potential  $\mu$  is lower than bulk liquid because of disjoining and capillary forces, therefore the vapour pressure ( $p_v$ ) decreases according to:

$$\frac{p_v}{p_0} = \exp(\Delta\mu/R_g T) \quad (6)$$

where  $p_0$  is the vapour pressure of bulk liquid,  $R_g$  is the ideal gas constant,  $T$  is the temperature and  $\Delta\mu$  is the increment of the chemical potential. The rate of evaporation,  $V_E$ , is proportional to the difference between  $p_v$  and the ambient vapour pressure,  $p_A$ :

$$V_E = k(p_v - p_A) \quad (7)$$

where  $k$  is a coefficient that depends on the design of the drying chamber, draft rate, etc. It appears reasonable to conclude that the surface of the body must be covered with a film of liquid (as in Fig. 6a), because the rate would decrease as the body shrinks if evaporation occurs only from the menisci, Fig. 6b.

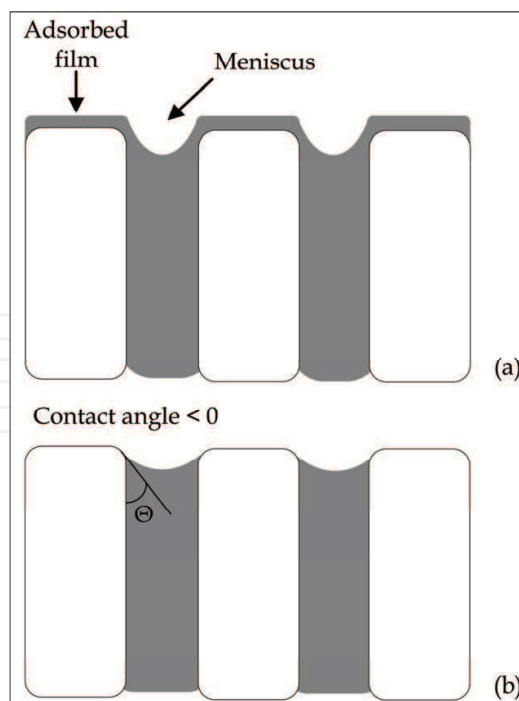


Fig. 6. Distribution of liquid at the surface of a drying porous body, when liquid is (a) spreading (contact angle  $\theta=0^\circ$ ) or (b) wetting, but not spreading ( $90^\circ > \theta > 0^\circ$ ). The chemical potential of the liquid in the adsorbed film is equal to that under the meniscus.

### 3. Experimental procedures

#### 3.1 Sol-gel synthesis of organic – inorganic hybrid materials

Hybrid organic-inorganic biomaterials were prepared by means of a sol-gel process from an analytical reagent grade of metal alkoxides  $M(OR)_x$  in an ethanol, organic polymer like poli- $\epsilon$ -caprolactone (PCL Mw = 65,000), water and solvent ( $CHCl_3$ ) mixture. Water, diluted with ethanol was added to the solution under a vigorous stirring. A flow-chart of hybrids ( $MO_2 + PCL \times wt\%$ ) can show the synthesis by the sol-gel method.  $MO_2/PCL$ , all mixed with drugs ( $y wt\%$ ), were also prepared by using an analytical reagent grade as a precursor material.

In this study  $SiO_2/PCL$  (PCL 0, 6, 12, 50 wt%) materials were used as support matrices for controlled drug release. Silica gel, originally developed for engineering applications, is also currently being studied as a polymer for the entrapment and sustained release of drugs (Teoli et al., 2006). In the present study the sol-gel method was applied to encapsulate Ketoprofen (5, 10, 15 wt%) as a model drug. The drug loaded amorphous bioactive materials were studied in terms of their drug release kinetics

The hybrid inorganic-organic materials (PCL 0, 6, 12, 50 wt%) were prepared by means of sol-gel process from an analytical reagent grade of tetraethyl orthosilicate (TEOS) in an ethanol, poly- $\epsilon$ -caprolactone (PCL), water, and chloroform ( $CHCl_3$ ) mixture. Water, diluted with ethanol was added to the solution under vigorous stirring. Fig. 7 shows the flow chart of hybrid ( $SiO_2 + \%PCL + \%Ketoprofen$ ) synthesis by the sol-gel method. As it is shown in the same Fig. 7,  $SiO_2/PCL$  (PCL 0, 6, 12, 50 wt%) all mixed with ketoprofen (5, 10, 15 %) were prepared by using an analytical reagent grade as precursor material.

After the addition of each reactant the solution was stirred and the resulting sols were uniform and homogeneous. The gelification time was controlled by varying the concentration of PCL, as shown in Tab. 4. After gelification the gels were air dried at  $50^\circ C$  for 24h to remove the residual solvent; as this treatment does not modify the stability of ketoprofen, glassy pieces were obtained (Fig. 8). Discs with a diameter of 13 mm and a thickness of 2 mm were obtained by pressing a fine ( $<125 \mu m$ ) gel powder into a cylindrical holder.

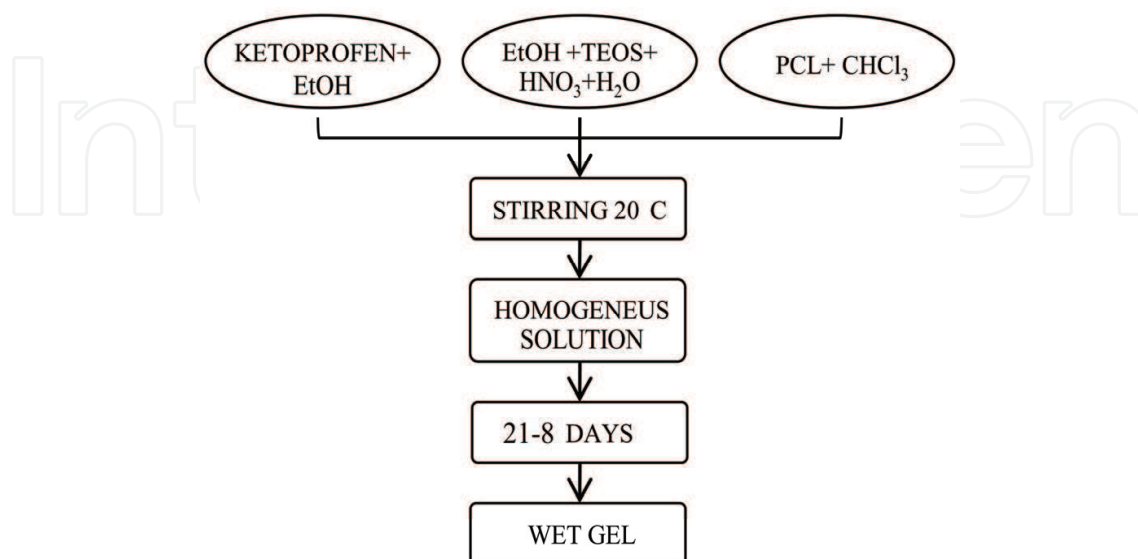


Fig. 7. Flow chart of  $SiO_2/PCL$  gel synthesis.

Materials prepared	Gelation time (20-25°C)
SiO <sub>2</sub> + 0%PCL + 5%Ketoprofen	21
SiO <sub>2</sub> + 6%PCL + 5%Ketoprofen	16
SiO <sub>2</sub> + 12%PCL + 5%Ketoprofen	14
SiO <sub>2</sub> + 50%PCL + 5%Ketoprofen	8
SiO <sub>2</sub> + 0%PCL + 10%Ketoprofen	19
SiO <sub>2</sub> + 6%PCL + 10%Ketoprofen	15
SiO <sub>2</sub> + 12%PCL + 10%Ketoprofen	12
SiO <sub>2</sub> + 50%PCL + 10%Ketoprofen	9
SiO <sub>2</sub> + 0%PCL + 15%Ketoprofen	18
SiO <sub>2</sub> + 6%PCL + 15%Ketoprofen	14
SiO <sub>2</sub> + 12%PCL + 15%Ketoprofen	12
SiO <sub>2</sub> + 50%PCL + 15%Ketoprofen	10

Table 4. Variation in the gelification time, controlled by changing the concentration of PCL.



Fig. 8. SiO<sub>2</sub>/PCL gel after drying.

Chromatographic experiments were carried out on a Shimadzu HPLC system, equipped with a Class-VP 5.0 software, an UV spectrophotometric detector SPD-10AVvp and two pumps LC-10ADvp, with low-pressure gradient systems. Samples of solutions were injected by a syringe via a Rheodyne loop injector; the loop volume was 20 µl, the analytical column was a Phenomenex C18 (150 × 4.60 mm; 5 µ); the flow rate of the mobile phase A (water) was set at 0.8 ml/min and that of the mobile phase B (methanol) was set at 0.2 ml/min. The total runtime was 10 minutes. HPLC grade methanol was obtained by Sigma-Aldrich. HPLC grade water was prepared using a Millipore (0.22 µm) system. A standard solution of ketoprofen 3 mM in a simulated body fluid (SBF) was prepared and the samples were taken at the end of the release from the materials.

The nature of SiO<sub>2</sub> gel, poly-ε-caprolactone (PCL) and PCL/SiO<sub>2</sub> hybrid materials were ascertained by X-ray diffraction (XRD) analysis using a Philips diffractometer. The presence of hydrogen bonds between organic-inorganic components of the hybrid materials was ascertained by FTIR analysis. Fourier transform infrared (FTIR) transmittance spectra were recorded in the 400-4000 cm<sup>-1</sup> region using a Prestige 21 Shimadzu system, equipped with a DTGS KBr (Deuterated Tryglycine Sulphate with potassium bromide windows) detector, with resolution of 2 cm<sup>-1</sup> (45 scans). KBr pelletized

disks containing 2 mg of sample and 200 mg KBr were made. The FTIR spectra were elaborated by IR solution software. The microstructure of the synthesized gels was studied by a scanning electron microscopy (SEM) Cambridge model S-240 on samples previously coated with a thin Au film and by a Digital Instruments Multimode atomic force microscopy (AFM) in contact mode in air.

3.2 Study of in vitro bioactivity

In order to study their bioactivity, samples of the studied hybrid materials were soaked in a simulated body fluid (SBF) with ion concentrations nearly equal to those of the human blood plasma, as reported elsewhere and shown in Tab. 5 (Hench & Clark, 1978; Ohtsuki et al., 1992; Paul, 1992). During soaking, the temperature was kept fixed at 37°C. Taking into account that the ratio of the exposed surface to the volume solution influences the reaction, a constant ratio of 50 mm<sup>2</sup> ml<sup>-1</sup> of solution was respected (Hutmacher et al., 2001).

Ion	Ions concentration (mM)	
	Human blood plasma	SBF
Na <sup>+</sup>	142.0	142.0
K <sup>+</sup>	5.0	5.0
Mg <sup>2+</sup>	1.5	1.5
Ca <sup>2+</sup>	2.5	2.5
Cl <sup>-</sup>	103.0	148.0
HCO <sub>3</sub> <sup>-</sup>	27.0	4.2
HPO <sub>4</sub> <sup>2-</sup>	1.0	1.0
SO <sub>4</sub> <sup>2-</sup>	0.5	0.5
pH	7.2 - 7.4	7.4

Table 5. Simulated body fluid (SBF) ionic concentration (mM).

It was shown that SBF reproduces *in vivo* bonelike apatite formation on bioactive glass and ceramic (Hench, 1991). *In vitro* studies using SBF have suggested that bioactive glass and glass-ceramics form bonelike apatite on their surface (see Fig. 9) by providing surface functional groups of silanol (Si–OH), which are effective for apatite nucleation. These groups combine with Ca<sup>2+</sup> ions present in the fluid imposing an increase of positive charge on the surface. In addition, Ca<sup>2+</sup> ions combine with the negative charge of the phosphate ions to form amorphous phosphate, which spontaneously transforms into hydroxyl-apatite [Ca<sub>10</sub>(PO<sub>4</sub>)<sub>6</sub>(OH)<sub>2</sub>] where the atomic ratio Ca/P is 1.60 (Ohtsuki et al., 1992). The SBF is already supersaturated with respect to the apatite under normal conditions. Once the apatite nuclei are formed, they can grow spontaneously by consuming the calcium and phosphate ions from the surrounding body fluid. It is known from literature (Hench, 1991; Ohtsuki et al., 1992) that CaO, SiO<sub>2</sub>-based glasses, CaO, P<sub>2</sub>O<sub>5</sub>- based glasses, sodium silicate glasses are more bioactive then ion free glass and ceramic. That is due to the dissolution of appreciable amounts of calcium and phosphate ions, which increase the degree of supersaturation of the surrounding body fluid with respect to the apatite. Moreover, the released ions are exchanged with H<sub>3</sub>O<sup>+</sup> ions in SBF forming silanol groups on their surface; this reaction causes a pH increase of SBF solution and, consequently, Si-OH groups are dissociated into negatively charged units Si-O<sup>-</sup> that interacts with the positively charged calcium ions to form the calcium silicate.

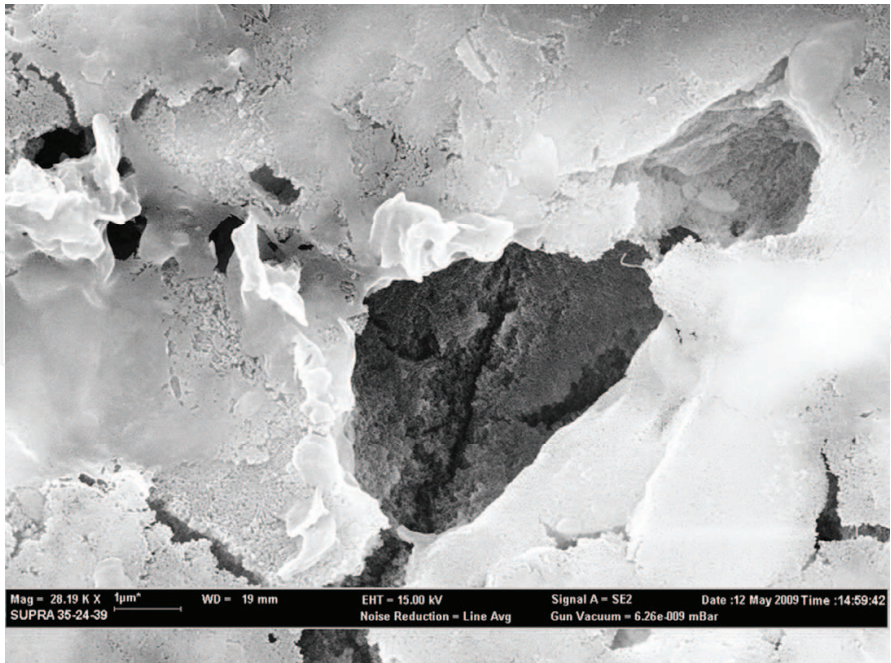


Fig. 9. Apatite layer on SiO<sub>2</sub>/PCL surface.

3.3 Study of in-vitro release

For the study of drug release, the discs of the investigated material were soaked in 15 ml of SBF, continuously stirred, at 37°C. The SBF was previously filtered with a Millipore (0.22 μm) system, to avoid any bacterial contamination. Drug release measurements were carried out by means of UV-VIS spectroscopy. Absorbance values were taken at a wavelength λ corresponding to an absorbance maximum value. The calibration curve was determined by taking absorbance versus drug concentration between 0 and 3 mM as parameters. For that interval the calibration curve fits the Lambert and Beers’ law (Wang & Pantano, 1992):

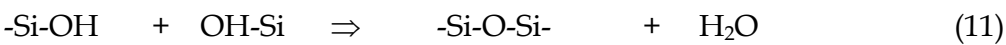
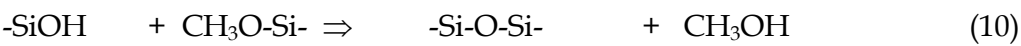
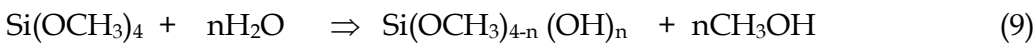
$$A = 1,26 \cdot C \tag{8}$$

where A is the absorbance and C is the concentration (mM).

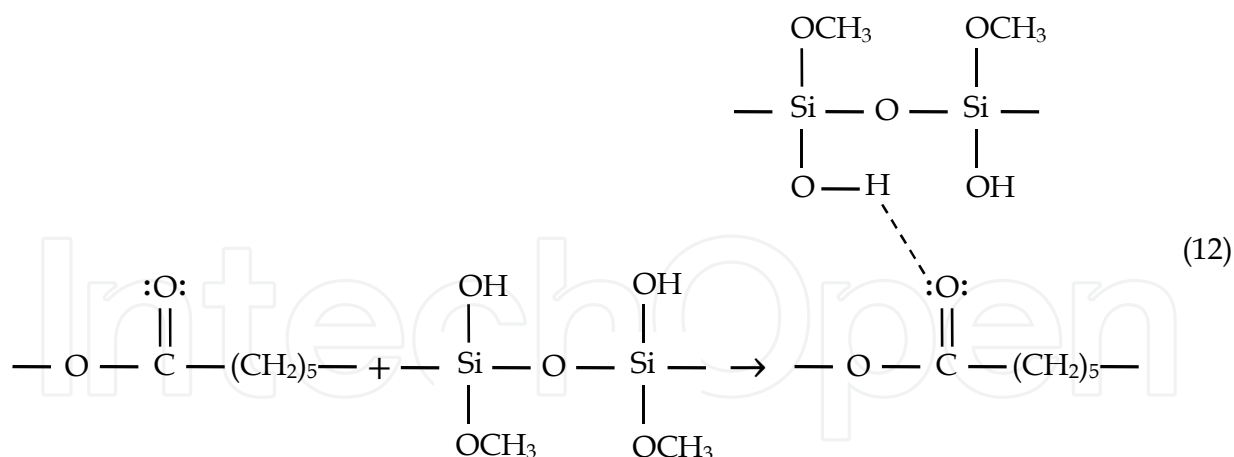
4. Characterization

4.1 Sol-gel characterization

Gelification is the result of hydrolysis and condensation reactions according to the following reactions:



Reaction 12 shows the formation of hydrogen bonds between the carbossilic group of organic polymer and the hydroxyl group of inorganic matrix.



The existence of hydrogen bonds was proved by FTIR measurements. Fig. 10 shows the infrared spectrum of the SiO<sub>2</sub> gel (Fig. 10a), the SiO<sub>2</sub>/PCL (6, 12, 50%wt) gels (Fig. 10b, 10c, 10d) and PCL (Fig. 10e). In Fig. 10a the bands between 3400 and 1600 cm<sup>-1</sup> are attributed to water (Sanchez & Ribot, 1994). The bands at 1080 and 470 cm<sup>-1</sup> are due to the stretching and bending modes of SiO<sub>4</sub> tetrahedra (Sanchez & Ribot, 1994). In the Fig. 10b, 10c, 10d and 10e, the bands at 2928 and 2840 cm<sup>-1</sup> are attributed to a symmetric stretching of -CH<sub>2</sub>- of polycaprolactone. The band at 1730 cm<sup>-1</sup> is due to the characteristic carboxylic group shifted to low wave numbers. The broad band at 3200 cm<sup>-1</sup> is the characteristic O-H group of hydrogen bonds.

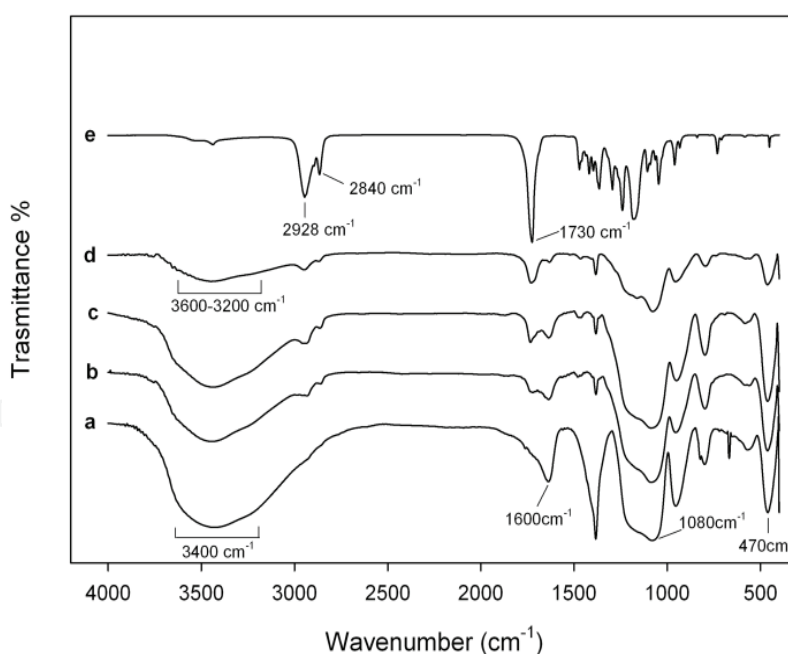


Fig. 10. FTIR of (a) SiO<sub>2</sub> gel, (b) SiO<sub>2</sub>+ PCL 6wt% (c) SiO<sub>2</sub>+ PCL 12wt% (d) SiO<sub>2</sub>+ PCL 50wt% gels and (e) PCL.

The nature and the microstructure of the hybrid materials have been studied by X-ray diffraction (XRD), scanning electron microscopy (SEM) and atomic force microscopy (AFM). The diffractograms in Fig. 11a show that SiO<sub>2</sub> gel exhibits the broad humps which are characteristic for amorphous materials, while the sharp peaks that can be detected on the

diffractogram of poly-ε-caprolactone and ketoprofen are typical of crystalline materials (Fig. 11b and 11c). On the other hand the XRD spectrum of hybrid SiO<sub>2</sub>/PCL exhibits the broad humps characteristic of amorphous materials (Fig. 11d), as well that of SiO<sub>2</sub> gel.

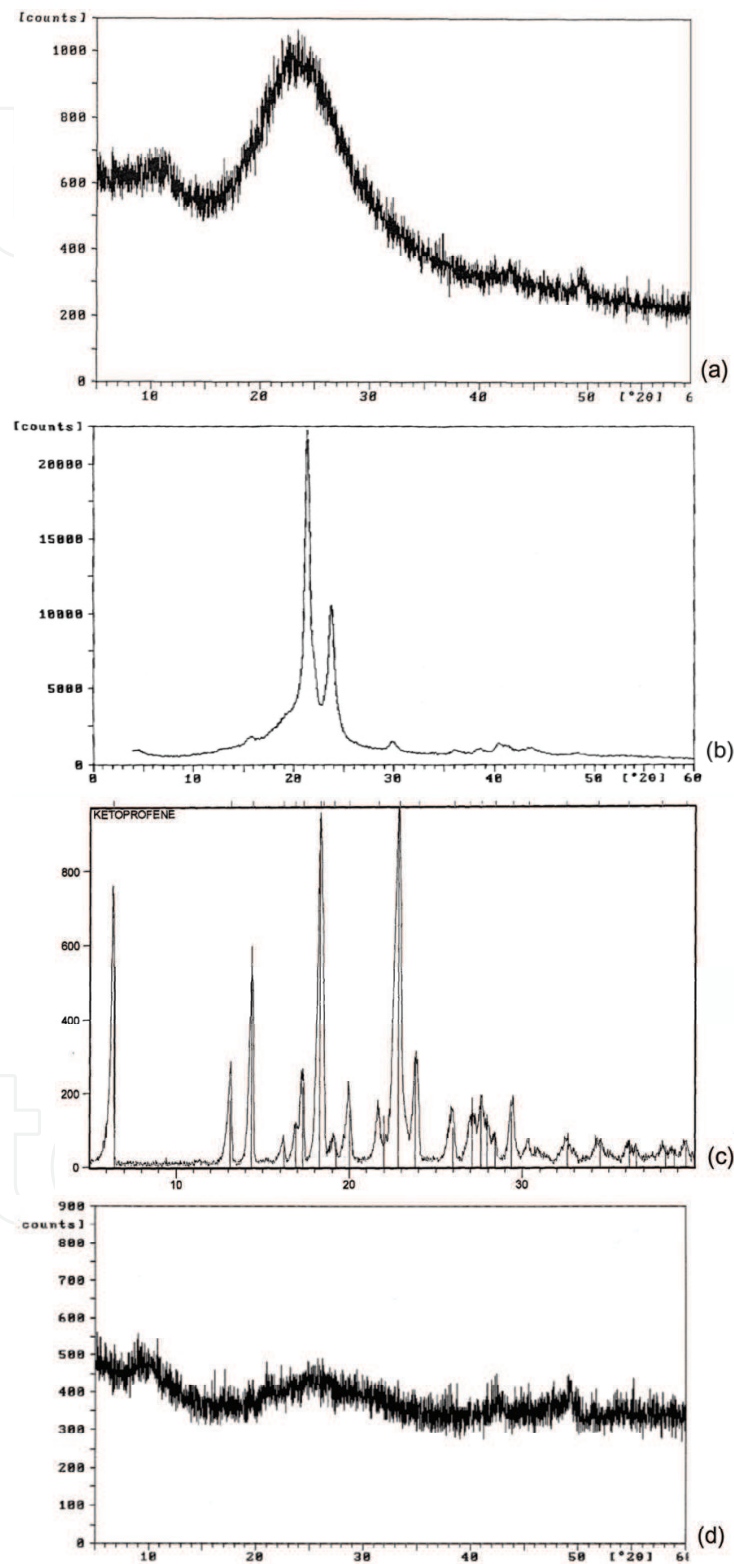


Fig. 11. XRD diffractogram of (a) SiO<sub>2</sub> gel, (b) PCL, (c) Ketoprofen, (d) SiO<sub>2</sub>/PCL gel.

SEM micrographs show that no appreciable difference can be observed between the morphology of the four amorphous materials. The samples appear as shown in Fig. 12. The degree of mixing of the organic-inorganic components, i. e. the phase homogeneity, has been ascertained by applying the atomic force microscopy (AFM) in the analysis of the sol-gel hybrid material.

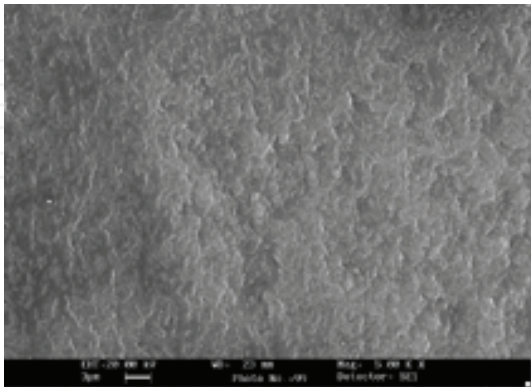


Fig. 12. SEM micrograph of SiO<sub>2</sub>/PCL gel.

The AFM contact mode image can be measured in the height mode or in the force mode. Force images (z range in nN) have the advantage that they appear sharper and richer in contrast and that the contours of the nanostructure elements are clearer. In contrast, height images (z range in nm) show a more exact reproduction of the height itself. In this work the height mode has been adopted to evaluate the homogeneity degree of the hybrid materials.

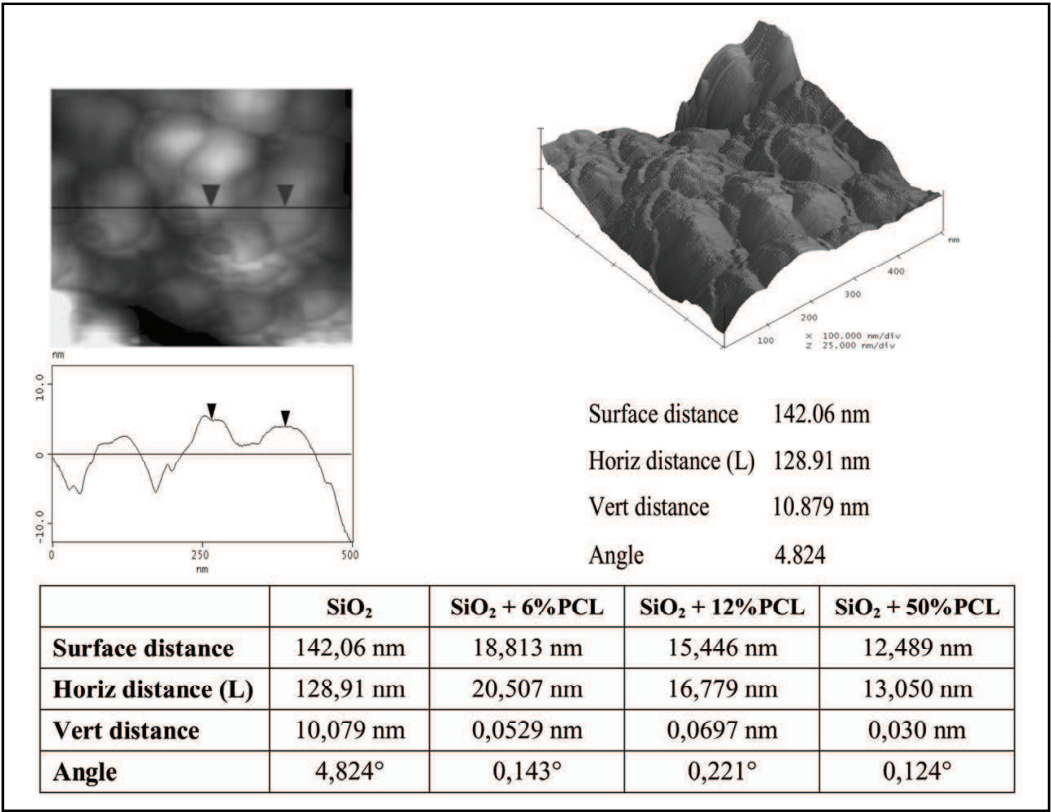


Fig. 13. AFM image showing the microstructure of SiO<sub>2</sub> gel .

The AFM topographic images of SiO<sub>2</sub> and SiO<sub>2</sub>/PCL (0, 6, 12, 50 wt%) gel samples are shown in Figs. 13 and 14. It can be observed that the average domain size is less than 130 nm. This result confirms that the synthesized PCL/SiO<sub>2</sub> gels can be considered organic-inorganic hybrid materials as suggested by literature data (Hench & Clark, 1978).

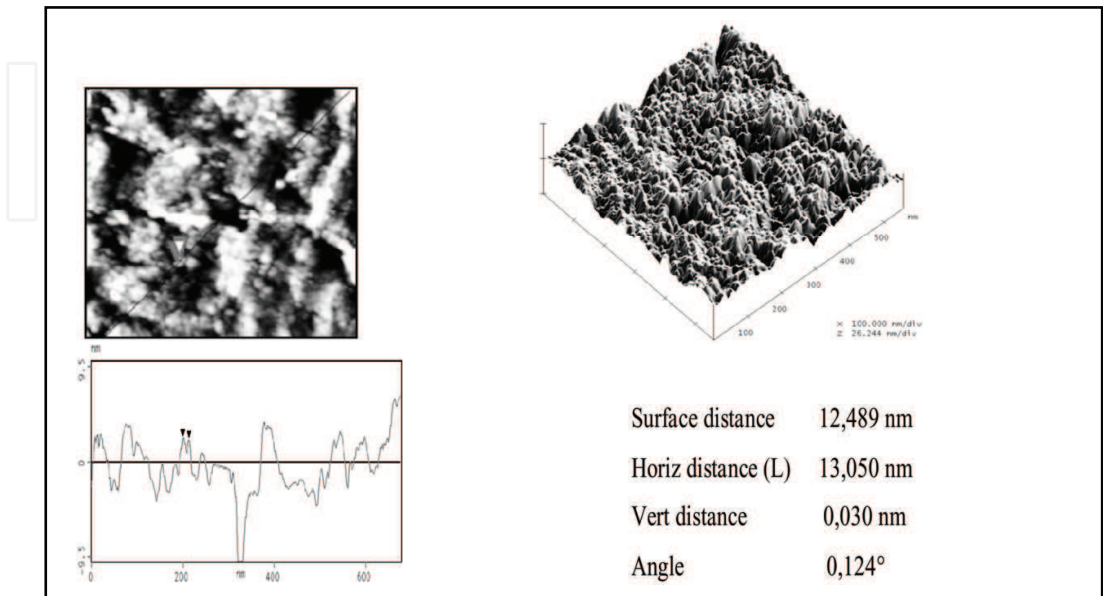


Fig. 14. AFM image showing the microstructure of SiO<sub>2</sub>/PCL gel.

4.2 Biological characterisation

The hybrid materials were soaked in SBF, as indicated by Ohtsuki et al. (1992), for in vitro bioactivity tests. The FTIR spectra after several exposures to SBF, 7, 14 and 21 days are shown in Fig. 15b, 15c and 15d. Evidence of the formation of an hydroxyapatite layer is given by the appearance of the 1116 and 1035 cm<sup>-1</sup> bands, usually assigned to P-O stretching (Teoli et al., 2006) and of the 580 cm<sup>-1</sup> band usually assigned to the P-O bending mode (Teoli et al., 2006). The splitting, already after a 7 day soaking, of the 580 cm<sup>-1</sup> band into two others at 610 and 570 cm<sup>-1</sup> can be attributed to formation of crystalline hydroxyapatite (Ohtsuki et al.). Finally the band at 800 cm<sup>-1</sup> can be assigned to the Si-O-Si band vibration between two adjacent tetrahedral, characteristic of silica gel (Teoli et al., 2006). These considerations support the hypothesis that a surface layer of silica gel forms as supposed in the mechanism proposed in the literature for hydroxyapatite deposition (Allen et al., 2000; Khor et al., 2002). Moreover an evaluation of the morphology of the apatite deposition and a qualitative elemental analysis were also carried out by electron microscopy observations on pelletized discs previously coated with a thin Au film. The EDS reported in Tab. 5 confirm that the surface layer observed in the SEM micrographs (Fig. 16) consists of calcium phosphate and which increases as the PCL.

Materials soaked in SBF for 21 days	Contents of Ca Atomic %	Contents of P Atomic %
SiO <sub>2</sub> + 0%PCL + Ketoprofen	2.65	1.64
SiO <sub>2</sub> + 6%PCL + Ketoprofen	3.13	1.94
SiO <sub>2</sub> + 12%PCL + Ketoprofen	5.04	3.23
SiO <sub>2</sub> + 50%PCL + Ketoprofen	7.82	4.86

Table 5. The EDS analyses of hybrid materials 21 days after immersion in SBF.

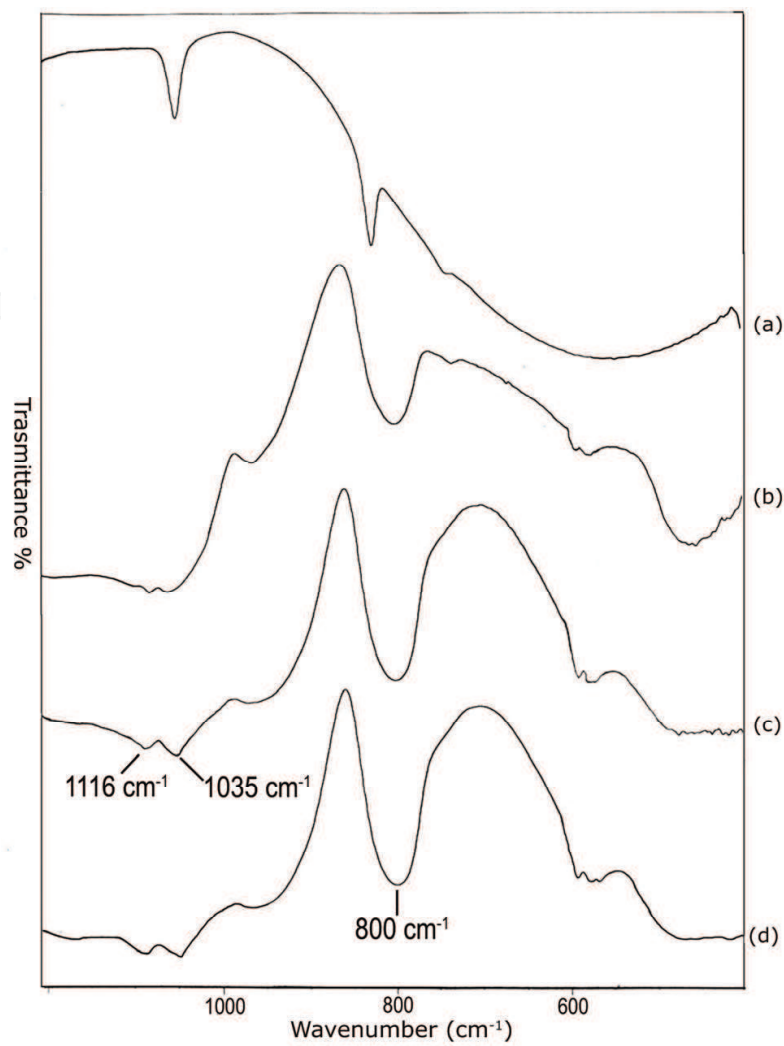


Fig. 15. FTIR spectra of SiO<sub>2</sub>/PCL gel samples after different times of exposure to SBF: (a) not exposed; (b) 7 days exposed;(c) 14 days exposed; (d) 21 days exposed.

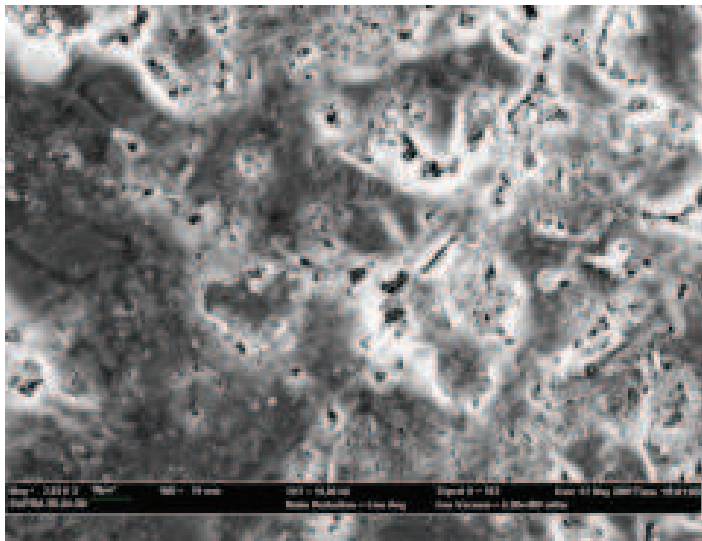


Fig. 16. SEM micrograph of SiO<sub>2</sub>/PCL gel after being exposed to SBF 21 days.

### 4.3 Release kinetic characterization

Kinetic measurements of release from the studied materials were carried out in 15 ml of SBF incubated at  $37 \pm 0.1^\circ\text{C}$  and under continuous magnetic stirring at 150 rpm. Sink conditions were maintained throughout all studies. The discs used were obtained with particle size between  $63\text{--}125\mu\text{m}$  compressed at 3 tons and aliquots of  $600\mu\text{l}$  were withdrawn at 1 h interval and replaced with an equal volume of release medium pre-equilibrated to temperature. Release was assayed by measuring the photometrical absorbance at 259.5 nm. In order to establish the relationship between the UV absorbance of at  $\lambda = 259.5\text{ nm}$  and the concentration of the solutions a calibration curve ( $r^2 = 0.9907$ ) was drawn for a standard solution with 4 levels of concentration: 0.0 mM, 1.0 mM, 2.0 mM and 3.0 mM (Fig. 17). All the standard solutions were prepared in SBF.

Fig. 18a, 19a, 20a and 18b, 19b, 20b show the drug release rates expressed as a percentage of the drug delivered, related to the drug-loading value, as a function of time. It was observed that from the  $\text{SiO}_2\text{+PCL}$  (0, 6, 12, 50 wt%)+ ketoprofen 5wt% gels about 60wt% of the drug was released in a relatively fast manner during the initial 2 hrs and it seems to be completed within 7 hrs without any evident difference in the time of release. For the  $\text{SiO}_2\text{+PCL}$ (0, 6, 12, 50 wt%)+ ketoprofen 10 and 15wt % gels about 60wt% of the drug was released during the initial 1 hr and 0,5 hr respectively and it is complete in about 3 hr and 4 hr respectively.

The differences observed in the release behaviour between  $\text{SiO}_2\text{+PCL}$  (0, 6, 12, and 50 wt%) + ketoprofen might be due to the different networks of the four gels that are determined by the different content percentage of PCL. The two stage release observed in all cases suggests that the initial stage of release occurs mainly by dissolution and diffusion of the drug entrapped close to or at the surface of the samples. The second and slower release stage involves the diffusion of the drug entrapped within the inner part of the clusters. An interesting observation is the general presence of an early lag period, which indicates the need for the penetration of the solvent into the structure. Fig. 18b, 19b and 20b show this particular kinetic describing the changes of the release speed during the two stages.

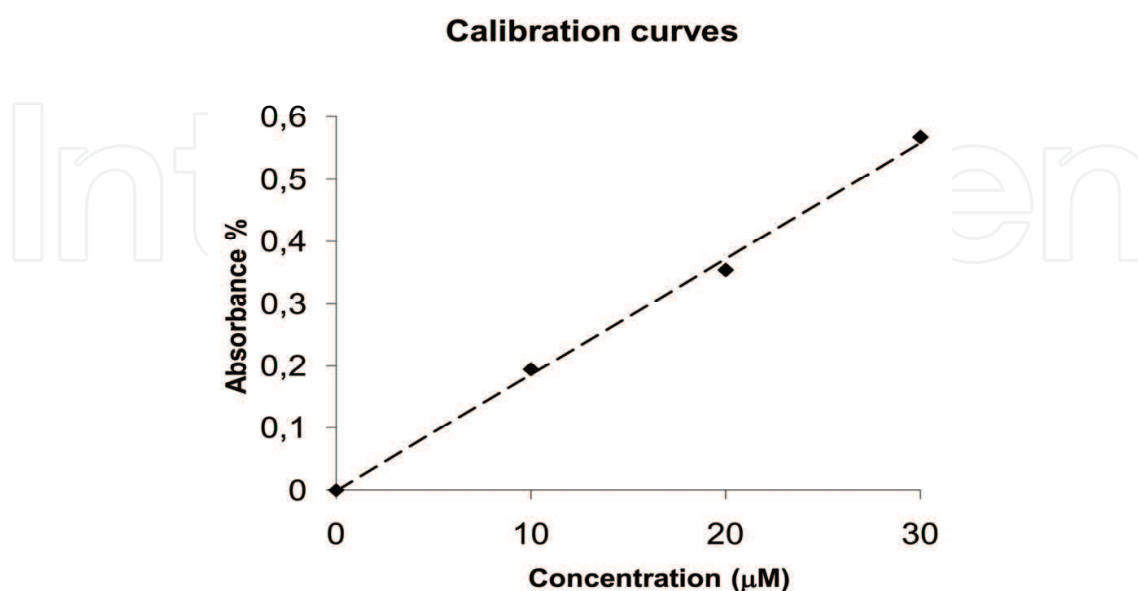


Fig. 17. Calibration curve (259.5 nm) depending on the concentration of Ketoprofen.

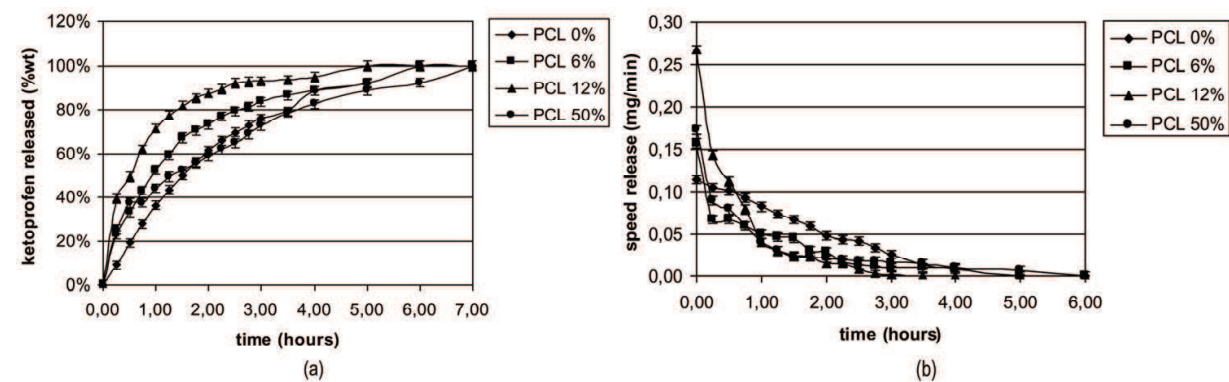


Fig. 18. (a) Time-dependent drug release plot for SiO<sub>2</sub> + PCL (0, 6, 12, 50%wt) + ketoprofen 5% at 37°C in SBF solution; (b) Time-dependent drug release rate plot for SiO<sub>2</sub> + PCL (0, 6, 12, 50%wt) + ketoprofen 5% at 37°C in SBF solution.

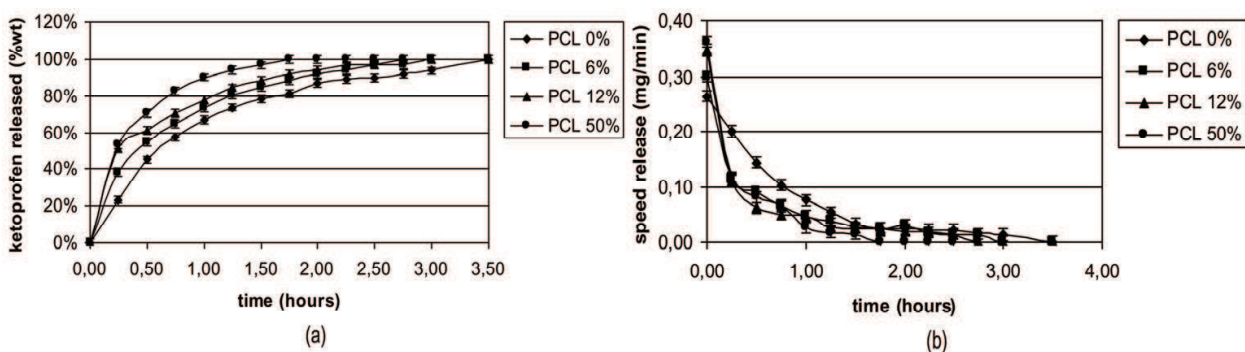


Fig. 19. (a) Time-dependent drug release plot for SiO<sub>2</sub> + PCL (0, 6, 12, 50%wt) + ketoprofen 10% at 37°C in SBF solution; (b) Time-dependent drug release rate plot for SiO<sub>2</sub> + PCL (0, 6, 12, 50%wt) + ketoprofen 10% at 37°C in SBF solution.

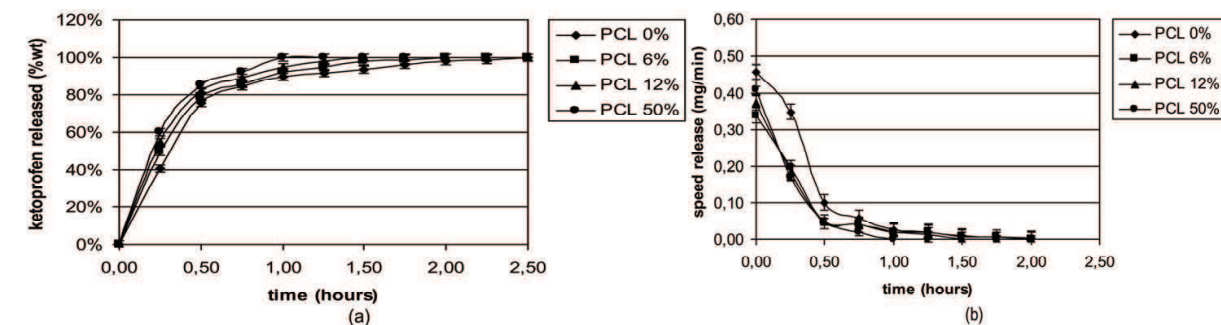


Fig. 20. (a) Time-dependent drug release plot for SiO<sub>2</sub> + PCL (0, 6, 12, 50%wt) + ketoprofen 15% at 37°C in SBF solution; (b) Time-dependent drug release rate plot for SiO<sub>2</sub> + PCL (0, 6, 12, 50%wt) + ketoprofen 15% at 37°C in SBF solution.

5. Applications

Applications for sol-gel processing derive from the various special shapes obtained directly from the gel state (e.g. monoliths, films, fibers, and monisized powders) combined with composition and microstructural control and low processing temperatures. Compared to conventional sources of ceramic raw materials, often minerals dug from the earth, synthetic

chemical precursors are a uniform and reproducible source of raw materials than can be made extremely pure through various synthetic means. Low processing temperatures, which result from microstructural control (e.g. high surface areas and small pore sizes), expand glass-forming regions by avoiding crystallization or phase separation, making new materials available to the technologist. The advantages of the sol-gel process (for preparing glass) are shown in Tab. 6 (Brinker & Scherer 1990). The disadvantages of sol-gel processing include the cost of the raw materials, shrinkage that accompanies drying and sintering, and processing time, as it is shown in Tab 7.

<ol style="list-style-type: none"><li>1. Better homogeneity from raw materials.</li><li>2. Better purity from raw materials.</li><li>3.Low temperature of preparation:<ol style="list-style-type: none"><li>a. Saving energy;</li><li>b. Minimizing evaporation losses;</li><li>c. Minimizing air pollution ;</li><li>d. No reactions with containers, thus purity;</li><li>e. Bypassing crystallization.</li></ol></li><li>4. New noncrystalline solids outside the range of normal glass formation.</li><li>5. New crystalline phases from new noncrystalline solids.</li><li>6. Better glass products from special properties of gel.</li><li>7. Special products such as film.</li></ol>
--

Table 6. Some advantages of the Sol-Gel Methods over Conventional Melting for Glass

<ol style="list-style-type: none"><li>1. High cost of raw materials.</li><li>2. Large shrinkage during processing.</li><li>3. Residual fine pores.</li><li>4. Residual hydroxyl.</li><li>5. Residual carbon</li><li>6. Health hazards of organic solution.</li><li>7. Long process time</li></ol>
---

Table 7. Some disadvantages of the Sol-Gel Methods

There are books (Klein, 1988) and a number of review papers (Dislich, 1986; Johnson, 1985; Klein & Garvey, 1982; Mackenzie, 1988; Uhlmann et al., 1984; Ulrich, 1988a) which discuss this topic in detail and whose primary purpose is to provide a source of references to current technology, and at the same time to analyze critical issues associated with the various classes of applications that must be addressed in order to advance the sol-gel technology; for example, a short outline can be as follows:

1. Thin films and coatings, which can be applied to optical, electronic, protective, and porous thin films or coatings. That represents the earliest commercial application of sol-gel technology.
2. Monoliths, i.e. applications for cast bulk shapes dried without cracking in such areas as optical components, transparent superinsulation, and ultralow-expansion glasses.
3. Powders, which can be used as ceramic precursors or abrasive grains and applications of dense or hollow ceramic or glass spheres.
4. Fibers, which are drawn directly from viscous sols and are used primarily for reinforcement or fabrication of refractory textiles.

5. Gels can also be used as matrices for fiber-, whisker-, or particle-reinforced composites and as host for organic, ceramic, or metallic phases.
6. Porous Gel; many applications exist which result from the ability to tailor the porosity of thin free-standing membranes, as well as bulk xerogels or aerogels.

In recent years interest in bioactive and biocompatibility of surface-active, biomaterials has grown.

Biomaterials have been used extensively in medical, personal care and food applications, with many similar polymers being used across disciplines. This perspective will emphasize hybrid materials used in medicine and specifically those designed as scaffolds for use in tissue engineering and regenerative medicine. The areas of active research in tissue engineering include: biomaterials design (incorporation of the appropriate chemical, physical, and mechanical/structural properties to guide cell and tissue organization); cell/scaffold integration (inclusion into the biomaterial scaffold of either cells for transplantation or biomolecules to attract cells, including stem cells, from the host to promote integration with the tissue after implantation); and biomolecule delivery (inclusion of growth factors and/or small molecules or peptides that promote cell survival and tissue regeneration). While a significant and growing area of regenerative medicine involves the stimulation of endogenous stem cells, this perspective will emphasize hybrid materials scaffolds used for delivery of cells and biomolecules. The challenges and solutions pursued in designing polymeric biomaterial scaffolds with the appropriate 3-dimensional structure are currently studied.

Ceramics and hybrid dioxide-based materials for the repairing of muscle-skeletal tissues are being increasingly applied over the last half century (Hench, 1991; Li, et al., 1996). Orthopaedic and maxillo-facial prosthesis provide evidence for the enhanced biomechanical performance of titanium and its alloys among metallic prosthetic components (Kitsugi et al., 1996).  $\text{TiO}_2$ -based bioactive ceramic suggests that bone grafting is achieved by supporting the precipitation of calcium (Ca) and phosphorus (P) into a structure similar to the mineral phase of bone. Accordingly, titanium is very promising to develop biomedical materials and devices designed as hard tissue substitutes with improved interface properties (Coreno & Coreno, et al. 2005; Hench, 1991; Li, et al., 1996; Kitsugi et al., 1996).

## 6. Conclusions

Sol-gel processing has attracted much attention, for the possibility that the method offers to new materials. We define sol-gel rather broadly as the preparation of glass, glass-ceramic and hybrid materials by a sol, its gelation and removal of the solvent. The sol-gel chemistry is based on the hydrolysis and polycondensation of molecular precursors such as metal alkoxides  $\text{M(OR)}_x$ , where  $\text{M} = \text{Si, Sn, Ti, Zr, Al, Mo, V, W, Ce}$  and so forth.

There are many potential applications of sol-gel derived materials in the form of films, fibers, monoliths, powders, composites, and porous media. The most successful applications are those that utilize the potential advantages of sol-gel processing such as purity, homogeneity, and controlled porosity combined with the ability to form shaped objects at low temperatures, avoiding inherent disadvantages such as costs of raw materials, slow processing times, and high shrinkage.

The  $\text{SiO}_2$  + PCL (0, 6, 12 and 50 %wt) materials, prepared via sol-gel process, were found to be organic - inorganic hybrid materials. The polymer (PCL) can be incorporated into the network by hydrogen bonds between the carboxylic groups of organic polymer and the hydroxyl groups of inorganic matrix. The release kinetics demonstrates that the investigated

materials supply high doses of the anti-inflammatory during the first hours when soaked in SBF and then a slower drug release allows a maintenance dose until the end of the experiment.

## 7. References

- Aelion, R., Loebel, A. & Eirich, F. (1950). Hydrolysis and polycondensation of tetraalkoxysilanes, *Recueil des Travaux Chimiques des Pays-Bas et de la Belgique*, Vol. 69, pp. 61-75, ISSN 0370-7539
- Aelion, R., Loebel, A. & Eirich, F. (1950). Hydrolysis of ethyl silicate, *Journal of the American Chemical Society*, Vol. 72, pp. 5705-5712, ISSN 0002-7863
- Allen, C., Han, J., Yu, Y., Maysinger, D. & Eisenberg, A. (2000). Polycaprolactone-*b*-poly(ethylene oxide) copolymer micelles as a delivery vehicle for dihydrotestosterone. *Journal of Controlled Release*, Vol. 63, No 3, pp. 275-286, ISSN 0168-3659
- Arcos, D., Ragel, C.V. & Vallet-Regí, M. (2001). Bioactivity in glass/PMMA composites used as drug delivery system, *Biomaterials*, Vol. 22, No. 7, pp. 701-708, ISSN 0142-9612
- Avnir, D. & Kaufman, V.R. (1987). Alcohol is an unnecessary additive in the silicon alkoxide sol-gel process, *Journal of Non-Crystalline Solids*, Vol. 92, No. 1, pp. 180-182, ISSN 0022-3093
- Black, J. & Hastings, G. (1998). *Handbook of Biomaterial Properties*, Chapman & Hall, ISBN 0412603306, New York, U.S.A.
- Brinker, C.J., Keefer, K.D., Schaefer, D.W. & Ashley, C.S. (1982). Sol-gel transition in simple silicates, *Journal of Non-Crystalline Solids*, Vol. 48, No. 1, pp. 47-64, ISSN 0022-3093
- Brinker, C.J. (1988). Hydrolysis and condensation of silicates: effects on structure, *Journal of Non-Crystalline Solids*, Vol. 100, No. 1-3, pp. 31-50, ISSN 0022-3093
- Ceaglske, N.H. & Hougen, O.A. (1937). Drying granular solids, *Journal of Industrial and Engineering Chemistry (Washington, D. C.)*, Vol. 29, pp. 805-813, ISSN 0095-9014
- Cogan, H.D. & Setterstrom, C.A. (1946). Properties of ethyl silicate, *Chemical & Engineering News*, Vol. 24, pp. 2499-2501, ISSN 0009-2347
- Coreno, J. & Coreno, O. (2005). Evaluation of calcium titanate as apatite growth promoter. *Journal of Biomedical Materials Research*, Vol. 75A, No. 2, pp. 478-84, ISSN 478-484
- Dislich, H. (1986). Sol-gel: science, processes and products, *Journal of Non-Crystalline Solids*, Vol. 80, No 1-3, pp.115-121, ISSN 0022-3093
- Dwivedi, R.K. (1986). Drying behavior of alumina gels, *Journal of Materials Science Letters*, Vol. 5, No. 4, pp. 373-376, ISSN 0261-8028
- Flory P.J. (1953). *Principles of Polymer Chemistry*, Cornell University Press, ISBN 0-8014-0134-8, Ithaca, New York
- Flory, P.J. (1974). Gels and gelling process, *Faraday Discussions of the Chemical Society*, Vol. 57, pp. 7-18, ISSN 0301-7249

- Fortes, M. & Okos, M. (1980). Drying Theories: Their Bases and Limitations as Applied to Foods and Grains, In: *Advances in Drying Vol 1*, A. Mujumdar (Ed.), 119-154, Hemisphere Publishing, ISBN 0070439753, New York, U.S.A.
- Gigant, K., Posset, U. & Schottner, G. (2002). FT-Raman spectroscopic study of the structural evolution in binary UV-curable vinyltriethoxysilane/tetraethoxysilane mixtures from the sol to the xerogel state, *Applied Spectroscopy*, Vol. 56, No. 6, pp. 762-769, ISSN 0003-7028
- Hench, L.L. & Clark, D.E. (1978). Physical chemistry of glass surfaces, *Journal of Non-Crystalline Solids*, Vol. 28, No. 1, pp. 83-105, ISSN 0022-3093
- Hench, L.L., Ortel, G. & Nogues, J.L. (1986). The role of chemical additives in sol-gel processing, *Materials Research Society Symposium Proceedings*, Vol. 73, No. Better Ceramic Chemistry 2, pp. 35-47, ISSN 0272-9172
- Hench, L.L. & West, J.K. (1990). The sol-gel process, *Chemical Reviews*, Vol. 90, No. 1, pp. 33-72, ISSN 0009-2665
- Hench, LL. (1991). Bioceramics: from concept to clinic, *Journal of American Ceramic Society*, Vol. 74, No. 7, pp. 1487-1510, ISSN 1551-2916.
- Hsiue, G.H., Kuo, J.K., Jeng, R.J., Chen, J.I., Jiang, X.L., Marturunkakul, S., Kumar, J. & Tripathy, S.K. (1994). Stable second-order nonlinear optical polymer network based on an organosoluble polyimide, *Chemistry of Materials*, Vol. 6, No. 7, pp. 884-887, ISSN 0897-4756
- Hutmacher, D.W., Schantz, T., Zein, I., Woei N.K., Hin T.S. & Cheng T.K. (2001). Mechanical properties and cell cultural response of polycaprolactone scaffolds designed and fabricated via fused deposition modeling, *Journal of Biomedical Materials Research*, Vol. 55, No. 2, pp. 203-216 ISSN 0021-9304
- Johnson, D.W.J. (1985). Sol-gel processing of ceramics and glass, *American Ceramic Society Bulletin*, Vol. 64, No. 12, pp. 1597-1602, ISSN 0002-7812
- Joshua, D.Y., Damron, M., Tang, G., Zheng, H., Chu, C.-J. & Osborne, J.H. (2001). Inorganic/organic hybrid coatings for aircraft aluminum alloy substrates. *Progress in Organic Coatings*, Vol. 41, No. 4, pp. 226-232, ISSN 0300-9440
- Judeinstein, P. & Sanchez, C. (1996). Hybrid organic-inorganic materials: a land of multidisciplinary, *Journal of Materials Chemistry*, Vol. 6, No. 4, pp. 511-525, ISSN 0959-9428
- Keefer, K.D. (1984). The effect of hydrolysis conditions on the structure and growth of silicate polymers, *Materials Research Society Symposium Proceedings*, Vol. 32, No. Better Ceramic Chemistry, pp. 15-24, ISSN 0272-9172
- Khor, H.L., Ng, K.W., Schantz, J.T., Phan, T.-T., Lim, T.C., Teoh, S.H. & Hutmacher, D.W. (2002). Poly( $\epsilon$ -caprolactone) films as a potential substrate for tissue engineering an epidermal equivalent. *Materials Science and Engineering: C*, Vol. 20, No. 1-2, pp. 71-75, ISSN 0928-4931
- Kitsugi, T., Nakamura, T., Oka, M., Yan, W.Q., Goto, T., Shibuya, T., Kokubo, T. & Miyaji, S. (1996). Bone bonding behavior of titanium and its alloys when coated with titanium oxide ( $\text{TiO}_2$ ) and titanium silicate ( $\text{Ti}_5\text{Si}_3$ ), *Journal of Biomedical Materials Reserch*, Vol. 32, No. 2, pp. 149-56, ISSN 1097-4636

- Klein, L.C. & Garvey, G.J. (1982). Silicon alkoxides in glass technology, *ACS Symposium Series*, Vol. 194, No. Soluble Silicon, pp. 293-304, ISSN 0097-6156
- Klein, L.C. (1988). *Sol-Gel Technology for Thin Films, Fibers, Preforms, Electronics and Specialty Shapes*, Noyes, ISBN 0-8155-1154-X, Park Ridge, New Jersey, U.S.A.
- Klukowska, A., Posset, U., Schottner, G., Wis, M.L., Salemi-Delvaux, C. & Malatesta, V. (2002). Photochromic hybrid sol-gel coatings: preparation, properties, and applications, *Materials Science*, Vol. 20, No. 1, pp. 95-104, ISSN 0137-1339
- Li, P., de Groot, K. & Kokubo, T. (1996). Bioactive  $\text{Ca}_{10}(\text{PO}_4)_6(\text{OH})_2\text{-TiO}_2$  composite coating prepared by sol-gel process. *Journal of Sol-gel Science and Technology*. Vol. 7, No. 1, pp. 27-34, ISSN 0928-0707
- Macey, H.H. (1942). Clay-water relationships and the internal mechanism of drying, *Transactions of the British Ceramic Society*, Vol. 41, pp. 73-120, ISSN 0371-5469
- Mackenzie, J.D. (1988). Applications of the sol-gel process. *Journal of Non-Crystalline Solids*, Vol. 100, No. 1-3, pp. 162-168, ISSN 0022-3093
- Mackenzie, J.D. & Bescher, E.P. (1998). Structures, properties and potential applications of Ormosils, *Journal of Sol-Gel Science and Technology*, Vol. 13, No. 1/2/3, pp. 371-377, ISSN 0928-070
- Matsuura, Y., Matsukawa, K., Kawabata, R., Higashi, N., Niwa, M. & Inoue, H. (2001). Synthesis of polysilane-acrylamide copolymers by photopolymerization and their application to polysilane-silica hybrid thin films, *Polymer*, Vol. 43, No. 4, pp. 1549-1553, ISSN 0032-3861
- Moore, F. (1961). Mechanism of moisture movement in clays with particular reference to drying-concise review, *Transactions of the British Ceramic Society*, Vol. 60, pp. 517-539, ISSN 0371-5469
- Morrison, R.T. & Boyd R.N. (1966). *Organic Chemistry*, Allyn & Bsacon, ISBN 0136436773, Boston, U.S.A.
- Novak, B.M. (1993). Hybrid nanocomposite materials - between inorganic glasses and organic polymers, *Advanced Materials*, Vol. 5, No. 6, pp. 422-433, ISSN 1521-4095
- Ohtsuki, C., Kokubo, T. & Yamamuro, T. (1992). Mechanism of apatite formation on  $\text{CaOSiO}_2\text{P}_2\text{O}_5$  glasses in a simulated body fluid. *Journal of Non-Crystalline Solids*, Vol. 143, No. 1, pp. 84-92, ISSN 0022-3093
- Paul, A. (1990). *Chemistry of Glasses*, Chapman and Hall, ISBN 0412230208, New York, U.S.A.
- Ragel, C.V. & Vallet-Regí, M. (2000). In vitro bioactivity and gentamicin release from glass-polymer-antibiotic composites, *Journal of Biomedical Materials Research*, Vol. 51, No. 3, pp. 424-429, ISSN 1552-4965
- Sanchez, C. & Ribot, F. (1994). Design of hybrid organic-inorganic materials synthesized via sol-gel chemistry. *New Journal of Chemistry*, Vol. 18, No. 10, pp. 1007-1047, ISSN 1144-0546
- Schmidt, H., Scholze, H. & Kaiser, A. (1984). Principles of hydrolysis and condensation reaction of alkoxysilanes, *Journal of Non-Crystalline Solids*, Vol. 63, No. 1-2, pp. 1-11, ISSN 0022-3093

- Shih, W.Y., Alkay, I.A. & Kikuchi, R. (1987), Phase diagrams of charged colloidal particles, *Journal of Chemistry and Physics*, Vol. 86, No. 9, pp. 5127-5132, ISSN 0021-9606
- Spanhel, L., Popall, G. & Muller, G. (1995). Spectroscopic properties of sol-gel derived nanoscaled hybrid materials, *Journal of chemical sciences*, Vol. 107, No. 6, pp. 637-644, ISSN 0974-3626
- Stauffer D., Coniglio A. & Adam M. (1982). Gelation and critical phenomena. *Advances in Polymer Science*, Vol. 44, No. Polymer Networks, pp. 103-158, ISSN 0065-3195
- Stockmayer W.H. (1945). *Advancing Fronts in Chemistry. Vol. 1. High Polymers*, Reinhold Publishing Company, New York, U.S.A.
- Stoeber, W., Fink, A. & Bohn, E. Controlled growth of monodisperse silica spheres in the micron size range, *Journal of Colloid and Interface Science*, Vol. 26, No. 1, pp. 62-69, ISSN 0021-9797
- Teoli, D., Parisi, L., Realdon, N., Guglielmi, M., Rosato, A. & Morpurgo, M. (2006). Wet sol-gel derived silica for controlled release of proteins, *Journal of Controlled Release*, Vol. 116, No. 3, pp. 295-303, ISSN 0168-3659
- Uhlmann, D.R., Zelinski, B.J.J. & Wnek, G.E. (1984). The ceramist as chemist - opportunities for new materials, *Materials Research Society Symposium Proceedings*, Vol. 32, No. Better Ceramics Through Chemistry, pp. 59-70, ISSN 0272-9172
- Ulrich, D.R. (1988). Prospects of sol-gel processes, *Journal of Non-Crystalline Solids*, Vol. 100, No. 1-3, pp. 174-193, ISSN 0022-3093
- Vallet-Regí, M., Ramila, A., del Real, R.P. & Perez-Pariente, J. (2000). A new property of MCM-41: drug delivery system, *Chemistry of Materials*, Vol. 13, No. 2, pp. 308-311, ISSN 0897-4756
- Vallet-Regí, M. (2001). Ceramics for medical applications, *Journal of the Chemical Society Dalton Transactions*, No. 2, pp. 97-108, ISSN 1472-7773
- Vallet-Regí, M. & Arcos, D. (2006). Nanostructured hybrid materials for bone tissue regeneration, *Current Nanoscience*, Vol. 2, No. 3, pp. 179-189
- Vallet-Regí, M. (2006). Bone repair and regeneration: possibilities, *Materialwissenschaft und Werkstofftechnik*, Vol. 37, No. 6, pp. 478-484, ISSN 1521-4052
- Vallet-Regí, M. (2006). Ordered mesoporous materials in the context of drug delivery systems and bone tissue engineering, *Chemistry - A European Journal*, Vol. 12, No. 23, pp. 5934-5943, ISSN 1521-3765
- Voronkov, M.G., Mileshekevich, V.P. & Yuzhelevskii, Y.A. (1978). *Studies in Soviet Science. The Siloxane Bond: Physical Properties and Chemical Transformations*, Consultants Bureau, ISBN 0306109409, New York, U.S.A.
- Wang, D.S. & Pantano, C.G. (1992). Surface chemistry of multicomponent silicate gels, *Journal of Non-Crystalline Solids Advanced Materials from Gels*, Vol. 147-148, pp. 115-122, ISSN 0022-3093
- Wei, Y., Xu, J., Dong, H., Dong, J.H., Qiu, K. & Jansen-Varnum, S.A. (1999). Preparation and physisorption characterization of d-glucose-templated mesoporous silica sol-gel materials, *Chemistry of Materials*, Vol. 11, No. 8, pp. 2023-2029, ISSN 0897-4756

- Zallen R. (1983). *The Physics of Amorphous Solids*, Wiley, ISBN 9783527602797, New York, U.S.A.
- Young, S.K., Gemeinhardt, G.C., Sherman, J.W., Storey, R.F., Mauritz, K.A., Schiraldi, D.A., Polyakova, A., Hiltner, A. & Baer, E. (2002). Covalent and non-covalently coupled polyester-inorganic composite materials, *Polymer*, Vol. 43, No. 23, pp. 6101-6114, ISSN . 0032-3861

IntechOpen

IntechOpen



## **Biomedical Science, Engineering and Technology**

Edited by Prof. Dhanjoo N. Ghista

ISBN 978-953-307-471-9

Hard cover, 902 pages

**Publisher** InTech

**Published online** 20, January, 2012

**Published in print edition** January, 2012

This innovative book integrates the disciplines of biomedical science, biomedical engineering, biotechnology, physiological engineering, and hospital management technology. Herein, Biomedical science covers topics on disease pathways, models and treatment mechanisms, and the roles of red palm oil and phytochemical plants in reducing HIV and diabetes complications by enhancing antioxidant activity. Biomedical engineering covers topics of biomaterials (biodegradable polymers and magnetic nanomaterials), coronary stents, contact lenses, modelling of flows through tubes of varying cross-section, heart rate variability analysis of diabetic neuropathy, and EEG analysis in brain function assessment. Biotechnology covers the topics of hydrophobic interaction chromatography, protein scaffolds engineering, liposomes for construction of vaccines, induced pluripotent stem cells to fix genetic diseases by regenerative approaches, polymeric drug conjugates for improving the efficacy of anticancer drugs, and genetic modification of animals for agricultural use. Physiological engineering deals with mathematical modelling of physiological (cardiac, lung ventilation, glucose regulation) systems and formulation of indices for medical assessment (such as cardiac contractility, lung disease status, and diabetes risk). Finally, Hospital management science and technology involves the application of both biomedical engineering and industrial engineering for cost-effective operation of a hospital.

### **How to reference**

In order to correctly reference this scholarly work, feel free to copy and paste the following:

Catauro Michelina and Bollino Flavia (2012). Synthesis and Characterization of Amorphous and Hybrid Materials Obtained by Sol-Gel Processing for Biomedical Applications, Biomedical Science, Engineering and Technology, Prof. Dhanjoo N. Ghista (Ed.), ISBN: 978-953-307-471-9, InTech, Available from: <http://www.intechopen.com/books/biomedical-science-engineering-and-technology/synthesis-and-characterization-of-amorphous-and-hybrid-materials-obtained-by-sol-gel-processing-for->

**INTeCH**  
open science | open minds

### **InTech Europe**

University Campus STeP Ri  
Slavka Krautzeka 83/A  
51000 Rijeka, Croatia  
Phone: +385 (51) 770 447  
Fax: +385 (51) 686 166

### **InTech China**

Unit 405, Office Block, Hotel Equatorial Shanghai  
No.65, Yan An Road (West), Shanghai, 200040, China  
中国上海市延安西路65号上海国际贵都大饭店办公楼405单元  
Phone: +86-21-62489820  
Fax: +86-21-62489821

[www.intechopen.com](http://www.intechopen.com)

IntechOpen

IntechOpen

© 2012 The Author(s). Licensee IntechOpen. This is an open access article distributed under the terms of the [Creative Commons Attribution 3.0 License](https://creativecommons.org/licenses/by/3.0/), which permits unrestricted use, distribution, and reproduction in any medium, provided the original work is properly cited.

IntechOpen

IntechOpen